An Analytical Solution for Inverse Determination of Residual Stress Field

S.A. Faghidian[1,*], G.H. Farrahi[2], D.J. Smith[3]

[1]Department of Mechanical and Aerospace Engineering, Science and Research Branch, Islamic Azad University, Tehran, Iran
[2]School of Mechanical Engineering, Sharif University of Technology, Tehran, Iran
[3]Department of Mechanical Engineering, University of Bristol, BS8 1TR, UK

ABSTRACT

An analytical solution is presented that reconstructs residual stress field from limited and incomplete data. The inverse problem of reconstructing residual stresses is solved using an appropriate form of the airy stress function. This function is chosen to satisfy the stress equilibrium equations together with the boundary conditions for a domain within a convex polygon. The analytical solution is demonstrated by developing a reference solution from which selected "measurement" points are used. An artificial error is then randomly added to "measurement" points for studying the stability of the reconstruction method utilizing Tikhonov-Morozov regularization technique. It is found that there is an excellent agreement between the model prediction and limited set of residual stress data in the sense of least-square approximation.
© 2012 IAU, Arak Branch. All rights reserved.

Keywords: Residual stress; Incomplete discrete data; Inverse problems; Approximation theory; Convex polygon domain

1 INTRODUCTION

RESIDUAL stresses are generated in engineering parts as a result of different manufacturing processes. Quantifying these residual stresses is a key step in determining the continued integrity and safety of a structure. This is because uncontrolled residual stresses are detrimental to the performance and lifetime of engineering components.

Quantifying the residual stress field in engineering structures can be classified by two approaches, the interpretation of experimental measurements and process modeling. Major limitations exist in both approaches; reliable process modeling requires exact characterization of material constitutive behavior and experimental measurements commonly result in limited and incomplete discrete data and usually only one component of the residual stress field is measured. The present study considers the second case, where there exists a limited and incomplete set of data. An analysis is developed to permit the complete distribution of residual stress field to be reconstructed.

Reconstruction of residual stress field from limited experimental measurements has been attempted previously by Smith et al. [1], utilizing experimental measurements in steel cylindrical bars that was hot forged and then shot blasted. Their method required that there was an assumed distribution of the plastic strain generated during shot blasting. This is equivalent to introducing an eigenstrain distribution to reconstruct the residual stresses. An eigenstrain approach to reconstruct residual stress field was first developed by Hill [2] in autofrettaged thick-walled tubes. Cao et al. [3] presented an inverse approach based on the inherent strain (eigenstrain) method for

___

determination of the residual stress field induced by welding, and used the finite element method to consider some typical examples. Also based on the inherent strain method, the boundary element method was utilized by Qian et al. [4] to reconstruct residual stress fields. More generally, an eigenstrain approach was developed by Korsunsky et al. [5] for thin welded plates. They used a finite element based formulation for determination of the distribution of eigenstrains in a welded plate from residual stress measurements. Recently, Jun and Korsunsky [6] proposed a general framework based on eigenstrain method using a finite element based formulation to reconstruct residual stresses. They applied an eigenstrain approach to a shot-peened sample and also friction stir welds. Ballard and Constantinescu [7], and Schajer and Prime [8] used approximate inverse methods to create the residual stress field. Theoretical work by Hoger [9], Mura and Gao [10] and Robertson [11] considered the hypothetical problem of recovering the residual stress in an elastic body from the measurements taken on the boundary of the body. However, they do not illustrate the application of their analysis. It is also interesting to note that Airy stress function was utilized by Moore and Evans [12] to correct the measured residual stress determined by X-ray diffraction and layer removal. They also obtained closed form solution based on airy stress function for simple geometry of domain and known nature of the residual stress distribution.

In contrast to earlier research, Faghidian [13] developed a new analytical method for reconstructing the residual stress field that does not require numerical tools such as the finite element or boundary element methods, or an assumed plastic strain or eigenstrain distribution. The new analytical approach determined the complete residual stress field utilizing an incomplete set of residual stress measurements by solving the stress equilibrium equations directly. The proposed method was then applied to a variety of examples, e.g. shot peening [14], autofrettaged thick-walled tubes [15], turning process [16], welded plates [17] and a rectangular beam subjected to elastic-plastic bending [18]. All of these examples are confined to specific geometric shapes and in this paper an analytical solution for a domain contained within a convex polygon is presented.

2 DETERMINATION OF THE RESIDUAL STRESS DISTRIBUTION
2.1 Governing equations

Residual stresses are defined as the stresses supported in a body in a fixed reference configuration where there is the absence of external forces and thermal gradients [9]. Thus, the residual stress field satisfies the equilibrium equations,

$$\nabla.\boldsymbol{\sigma} = 0$$
$$\boldsymbol{\sigma} = \boldsymbol{\sigma}^T \tag{1}$$

on the volume of the body B. The free traction surface conditions are:

$$\boldsymbol{\sigma}.\mathbf{n} = 0 \tag{2}$$

on its boundary ∂B, where n is the outward unit normal. Further insight into the residual stress is gained by determining its volume average,

$$\boldsymbol{\sigma}_M(B) = \frac{1}{V(B)} \int_B \boldsymbol{\sigma} dV \tag{3}$$

where $V(B)$ is the volume of body B. The mean stress theorem states [19]:

$$\boldsymbol{\sigma}_M(B) = \frac{1}{V(B)} \left[\int_{\partial B} (\mathbf{r} - \mathbf{r_0}) \otimes (\boldsymbol{\sigma}.\mathbf{n}) dA - \int_B (\mathbf{r} - \mathbf{r_0}) \otimes (\nabla.\boldsymbol{\sigma}) dV \right] \tag{4}$$

where r is the position vector and r_0 is a fixed reference point. Consequently, with Eq. (1) and Eq. (2),

$$\boldsymbol{\sigma}_M(B) = 0 \tag{5}$$

i.e., the Cartesian components of mean residual stress are always zero.

Now the plane condition is considered, i.e., it is assumed that all residual stresses and strains are independent of coordinate z that is an outward normal to the plane. The governing equilibrium equations are [19]:

$$\frac{\partial \sigma_{xx}}{\partial x} + \frac{\partial \sigma_{xy}}{\partial y} = 0, \quad \frac{\partial \sigma_{xy}}{\partial x} + \frac{\partial \sigma_{yy}}{\partial y} = 0 \tag{6}$$

The geometry of the domain for the analytical solution is considered to be a regular convex polygon shape, shown in Fig. 1. The boundary conditions include zero traction on the outer sides, and are:

$$\sigma_n^i = 0, \tau_i = 0 \quad on \quad y = m_i x + b_i \tag{7}$$

where $y = m_i x + b_i$ is the line equation of i-th side. Also, if $\vec{\mathbf{n}} = n_i \hat{e}_i$ represents the outward unit normal of the i-th side and the Cartesian components of residual stress field are given by $\boldsymbol{\sigma} = \sigma_{ij} \hat{e}_i \otimes \hat{e}_j$, then the normal and shear traction on this side, respectively σ_n and τ, are [19]:

$$\sigma_n = n_i \sigma_{ij} n_j$$
$$\tau = \sqrt{\sigma_i \sigma_i - \sigma_n^2} = \sqrt{\left(n_j \sigma_{ij}\right)\left(n_k \sigma_{ik}\right) - \left(n_i \sigma_{ij} n_j\right)^2} \tag{8}$$

A further condition is that:

$$\iint_A \sigma_{ij} dA = 0 \tag{9}$$

where A is the area of the convex polygon.

It is now appropriate to introduce an airy stress function, $\varphi(x, y)$ that satisfies the equilibrium equations Eq. (6), where [19]:

$$\sigma_{xx}(x, y) = \frac{\partial^2 \varphi(x, y)}{\partial y^2}, \quad \sigma_{xy}(x, y) = -\frac{\partial^2 \varphi(x, y)}{\partial x \partial y}, \quad \sigma_{yy}(x, y) = \frac{\partial^2 \varphi(x, y)}{\partial x^2} \tag{10}$$

It now remains to ensure that traction free boundary conditions, Eqs. (7- 8), and the condition of a zero mean residual stress, Eq. (9), are satisfied. Let us introduce an airy stress function of the form:

$$\varphi(x, y) = f(x) g(y) \prod_{i=1}^{M} \left[y_i - \left(m_i x + b\right)\right]^2 \tag{11}$$
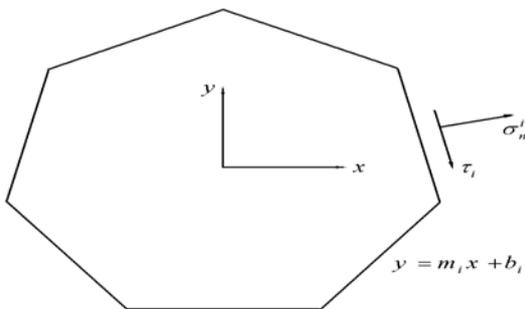
Fig. 1
Geometry of the arbitrary convex polygon for general solution.
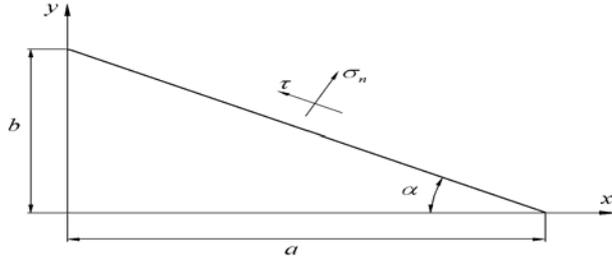
Fig. 2
Arbitrary side of the convex polygon.

where M is the number of the sides of the convex polygon and $f(x)$, $g(y)$ are arbitrary smooth analytical functions which should be at least $f(x)$, $g(y) \in C^2$, where C^2 is the set of functions that is continuous and doubly differentiable in the domain of the convex polygon. This choice of airy stress function not only satisfies all the continuum requirements but also results in a smooth nonsingular stress field. Also note that because of the existence of a plastic strain field in the continuum, in contrast to linear elastic problems, the airy stress function does not need to be bi-harmonic.

To prove this, let us consider an arbitrary side of the convex polygon, shown in Fig. 2. It is shown that when the traction stresses, σ_n and τ, are zero on the inclined face, then the convex polygon will be traction free. To illustrate this, the following airy stress function that is rearrangement of the Eq. (11):

$$
\begin{aligned}
\varphi(x,y) &= (y + x \tan\alpha - b)^2 f(x) g(y) \prod_{i=1}^{M-1} \left[y_i - (m_i x + b) \right]^2 \\
&= (y + x \tan\alpha - b)^2 F(x,y)
\end{aligned}
$$

(12)

Introducing Eq. (12) in Eq. (10) results in a smooth nonsingular form of the residual stress field given by:

$$
\sigma_{xx}(x,y) = 2F(x,y) + 4(y + x \tan\alpha - b)\frac{\partial F(x,y)}{\partial y} + (y + x \tan\alpha - b)^2 \frac{\partial^2 F(x,y)}{\partial y^2}
$$

$$
\begin{aligned}
\sigma_{yy}(x,y) &= 2F(x,y)\tan^2\alpha + 4\tan\alpha(y + x \tan\alpha - b)\frac{\partial F(x,y)}{\partial x} \\
&\quad + (y + x \tan\alpha - b)^2 \frac{\partial^2 F(x,y)}{\partial x^2}
\end{aligned}
$$

(13)

$$
\begin{aligned}
\sigma_{xy}(x,y) &= -2F(x,y)\tan\alpha + (y + x \tan\alpha - b)\left[-2\left(\tan\alpha \frac{\partial F(x,y)}{\partial y} + \frac{\partial F(x,y)}{\partial x} \right) \right] \\
&\quad - (y + x \tan\alpha - b)\frac{\partial^2 F(x,y)}{\partial x \partial y}
\end{aligned}
$$

The tractions on the inclined face is derived by re-writing Eq. (8) as:

$$
\begin{aligned}
\sigma_n &= n_i \sigma_{ij} n_j = \sigma_{xx} \sin^2\alpha + \sigma_{xy} \sin 2\alpha + \sigma_{yy} \cos^2\alpha \\
\tau &= \sqrt{\sigma_i \sigma_i - \sigma_n^2} = \sqrt{(n_j \sigma_{ij})(n_k \sigma_{ik}) - (n_i \sigma_{ij} n_j)^2} \\
&= \frac{1}{2}\left[\sin 2\alpha(\sigma_{xx} - \sigma_{yy}) + 2\sigma_{xy} \cos 2\alpha \right]
\end{aligned}
$$

(14)

Utilizing Eq. (13) in Eq. (14) and performing parametric mathematical simplifications, gives:

$$\sigma_n = (y + x \tan \alpha - b)^2 \left[\sin^2 \alpha \frac{\partial^2 F(x,y)}{\partial y^2} - 2 \sin \alpha \cos \alpha \frac{\partial^2 F(x,y)}{\partial x \partial y} + \cos^2 \alpha \frac{\partial^2 F(x,y)}{\partial x^2} \right]$$

$$\tau^2 = \frac{1}{2}(y + x \tan \alpha - b) \left[4 \tan \alpha \frac{\partial F(x,y)}{\partial y} - 4 \frac{\partial F(x,y)}{\partial x} \right.$$
$$\left. - (y + x \tan \alpha - b) \left(2 \cos 2\alpha \frac{\partial^2 F(x,y)}{\partial x \partial y} + \sin 2\alpha \left(\frac{\partial^2 F(x,y)}{\partial x^2} - \frac{\partial^2 F(x,y)}{\partial y^2} \right) \right) \right] \qquad (15)$$

It can be seen that with $y + x \tan \alpha - b = 0$ the traction free boundary conditions, Eq. (7), are satisfied on the inclined side of the convex polygon. Consequently, the convex polygon will also be traction free. Furthermore, every Cartesian component of stress field in the domain must have a zero mean stress.

To control the behavior of the solution, ensuring the existence of an approximate solution and to make sure there is a unique solution, the arbitrary functions $f(x)$, $g(y)$ must have an asymptotic expansion. The airy stress function, Eq. (11), can be written as,

$$\varphi(x,y) = \left[\sum_{i=1}^{P} \sum_{j=1}^{Q} \left(c_{ij} f_i(x) g_j(y) \right) \right] \prod_{k=1}^{M} \left[y_k - (m_k x + b) \right]^2 \qquad (16)$$

where c_{ij} are the unknown real coefficients to be determined later. Once again, the shape functions for $f_i(x)$, $g_j(y)$ should be at least doubly differentiable in the domain of the convex polygon.

This approach is found to be adequate for a range of processes that induce residual stress, but the result depends on appropriate choice of shape functions. To choose the best form of the shape functions, the type of process, such as welding and shot peening should be known. Further details are given in Farrahi et al. [14-17], where different shape functions are selected to reflect the nature of the residual stress distribution.

It is also interesting to note that the equilibrium equations of stress, Eq. (6), are solved directly and there is no assumption on the strain field, so the reconstruction procedure can be applied successfully to both plane-stress and plane-strain conditions.

2.2 Least squares approximation

To achieve the best values for the real coefficients of c_{ij} that appear in the asymptotic expansion Eq. (16), a least squares approximation approach can be utilized to examine all components of the residual stress field. However, not all components of the residual stress tensor are measured throughout the entire domain of engineering part and typically only limited measurements of one component are made [15]. Without loss of generality, let us consider that only the stress, σ_{yy}, is "measured". Its asymptotic expansion is achieved, utilizing Eq. (16) in Eq. (10). For brevity, the stress σ_{yy} is considered to have the following compact form

$$\sigma_{yy}(x,y) = \sum_{i=1}^{P} \sum_{j=1}^{Q} c_{ij} \Upsilon_{ij}(x,y) \qquad (17)$$

Evaluating the function $\Upsilon_{ij}(x,y)$ at each of the k measurement points at coordinates (x_k, y_k) results in predicted values $\Upsilon_{ijk} = \Upsilon_{ij}(x_k, y_k)$. The corresponding values of the stress, σ_{yy} at (x_k, y_k) deduced from the measurements are denoted by T_k. The application of a weight function $w(x,y)$ at each k measurement results in predicted values $w_k = w(x_k, y_k)$. For a least square analysis of the stress, σ_{yy} the following function is introduced,

$$J = \sum_{k=1}^{N} w_k \left(\sum_{i=1}^{P} \sum_{j=1}^{Q} c_{ij} \Upsilon_{ijk} - T_k \right)^2 \tag{18}$$

where N is the number of measurements while P and Q are the numbers of truncated series used to approximate the residual stress field in x and y direction respectively. The form of the weight function $w(x,y)$ can be selected using the accuracy of measurement at different points. The weight function should be positive and (Riemann) integrable. No other restrictions exist [20].

It can be shown that unique values of the coefficients c_{ij} can be found as the solution of the following system,

$$\sum_{m=1}^{P} \sum_{n=1}^{Q} c_{mn} \Psi_{ijmn} = \Gamma_{ij} \tag{19}$$

where

$$\Psi_{ijmn} = \sum_{q=1}^{N} w_q \Upsilon_{ijq} \Upsilon_{mnq}, \quad \Gamma_{ij} = \sum_{q=1}^{N} w_q \Upsilon_{ijq} T_q \tag{20}$$

Because of the complexity of dealing with tensors with more than two dimensions, a linear map that reduces the order of the tensors appearing in Eq. (20) is defined and used. More details are given by Farrahi et al. [17]. Also further details of the mathematical formulation and the proof of invertibility and uniqueness of the approximate solution in the sense of a least square approximation are given in Cheney [20] and Groetsch [21].

3   RECONSTRUTION OF A SIMULATED RESIDUAL STRESS FIEL

To illustrate the power and flexibility of the method proposed in this paper, a triangular domain, shown in Fig. 2, is considered as a special case of an arbitrary convex polygon. For this triangular domain the airy stress function, Eq. (16), can be written as:

$$\varphi(x,y) = \left[\sum_{i=1}^{P} \sum_{j=1}^{Q} \left(c_{ij} f_i(x) g_j(y) \right) \right] \left[xy \left(y + x \tan\alpha - b \right) \right]^2 \tag{21}$$

The residual stress field is found by introducing Eq. (21) into Eq. (10). Solutions for the in-plane residual stresses are:

$$\sigma_{xx}(x,y) = \sum_{i=1}^{P} \sum_{j=1}^{Q} c_{ij} \left\{ x^2 f_i(x) \left[2 g_j(y) \left(b^2 - 6by + 6y^2 + x \tan\alpha (-2b + 6y + x \tan\alpha) \right) \right] \right.$$
$$\left. + y \left(-b + y + x \tan\alpha \right) \left[(-4b + 8y + 4x \tan\alpha) g_j'(y) + y \left(-b + y + x \tan\alpha \right) g_j''(y) \right] \right\}$$

$$\sigma_{xy}(x,y) = \sum_{i=1}^{P} \sum_{j=1}^{Q} c_{ij} xy \left\{ \left(-b + y + x \tan\alpha \right) f_i'(x) \left[g_j(y) (-2b + 4y + 2x \tan\alpha) \right] \right.$$
$$+ y \left(-b + y + x \tan\alpha \right) g_j'(y) - 2 f_i(x) \left[g_j(y) \left[2(b - 2y)(b - y) + x \tan\alpha (-6b + 9y + 4x \tan\alpha) \right] \right.$$
$$\left. + y \left(-b + y + x \tan\alpha \right) \left(-b + y + 2x \tan\alpha \right) g_j'(y) \right\} \tag{22}$$

$$\sigma_{yy}(x,y) = \sum_{i=1}^{P} \sum_{j=1}^{Q} c_{ij} \left\{ y^2 g_j(y) \left[2x^2 f_i(x) \tan^2\alpha + 4x \tan\alpha \left(-b + y + x \tan\alpha \right) \right. \right.$$
$$\left. \left. \times \left(2 f_i(x) + x f_i'(x) \right) + \left(-b + y + x \tan\alpha \right)^2 \left[2 f_i(x) + x \left(4 f_i(x) + x f_i''(x) \right) \right] \right] \right\}$$

In the following, a reference residual stress field is created within the triangular domain. One component of reference field is then treated as the measured stresses and then the analysis developed in this paper is used to

reconstruct the measured reference field and the other components that have not been measured. The reference airy function is defined by

$$\overline{\Phi}(x,y) = \left[xy\left(y + x\tan\alpha - b\right)\right]^2 \left[10^3 \exp\left(-0.5x\right)\exp\left(-y\right)\right] \tag{23}$$

Comparing Eq. (23) with Eq. (11), it is clear that the assumed reference airy stress would result in reference residual stress field that certainly satisfy all of the continuum mechanics requirements.

Also it should be noted that, there exists no analytical solution for residual stress distribution in convex polygon domains. So to compare the results of the reconstruction analysis with a reference solution and to study the effect of the artificially introduced errors, the reference airy stress function as Eq. (23) is introduced and utilized here.

It is assumed that only the magnitude of the stress, σ_{yy} of the reference residual stress field is known along four lines at equi-distant points. The dimensions of the geometry, $\left(a = 2,\ b = 1\right)$, and the location of the measurement points are illustrated in Fig. 3.
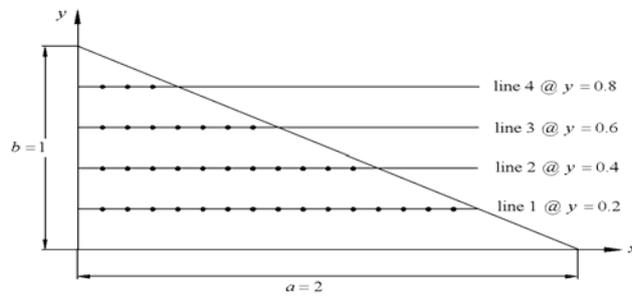
Fig. 3
Considered geometry and the location of the measurement points.

As indicated earlier, the shape functions $f_i(x)$ and $g_j(y)$ should be chosen to reflect the characteristics of the residual stress distribution with respect to the processes that introducing residual stresses to the domain. However, the reference residual stress does not show any familiar behavior and there is no symmetry in the domain. So, as a first approximation for both shape functions, $f_i(x)$ and $g_j(y)$ it is assumed that they are modified Chebyshev polynomials of the second kind given by:

$$\begin{aligned} f_i(x) &= T_{(i-1)}(x) \\ g_j(y) &= T_{(j-1)}(y) \end{aligned} \tag{24}$$

A least square approximation analysis, as developed in section 2.2, is used to achieve the best values for the coefficients of c_{ij} appearing in the asymptotic expansion, Eq. (22). Once the coefficients c_{ij} are determined, the complete residual stress field distribution given by Eq. (22) is reconstructed. The terms P, Q used in Eq. (22) are P =10 and Q=7, for both cases of reconstruction using either "Measured" values or "Realistic data".

"Measured" values and "Realistic data" of the residual stress, σ_{yy}, together with the reference residual stress distribution along lines 1 through 4 are shown in Fig. 4. The "Realistic data" obtained by randomly adding artificial absolute error to "Measured" values to simulate the experimental error. The artificial absolute error is ±10% of the maximum of all measurements.
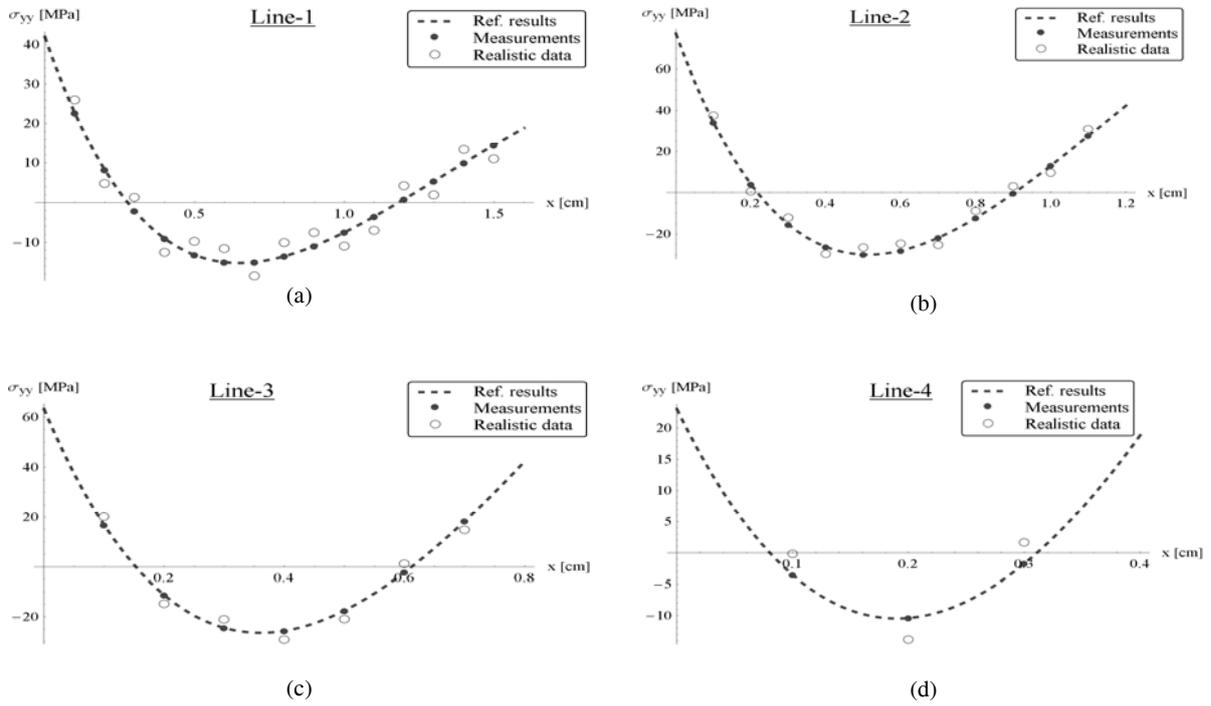
Fig. 4
"Measured" and "Realistic" values of the residual stress together with its reference residual stress distribution along lines 1 through 4.

The reconstructed residual stresses utilizing "Measured" data are shown in Fig. 5 and essentially are the same as the reference stress profile. The maximum error between the reconstructed residual stress using "Measured data", σ_{yy}, and the reference profile is 10^{-1} (MPa) that occurs along line-4.

(c)

(d)
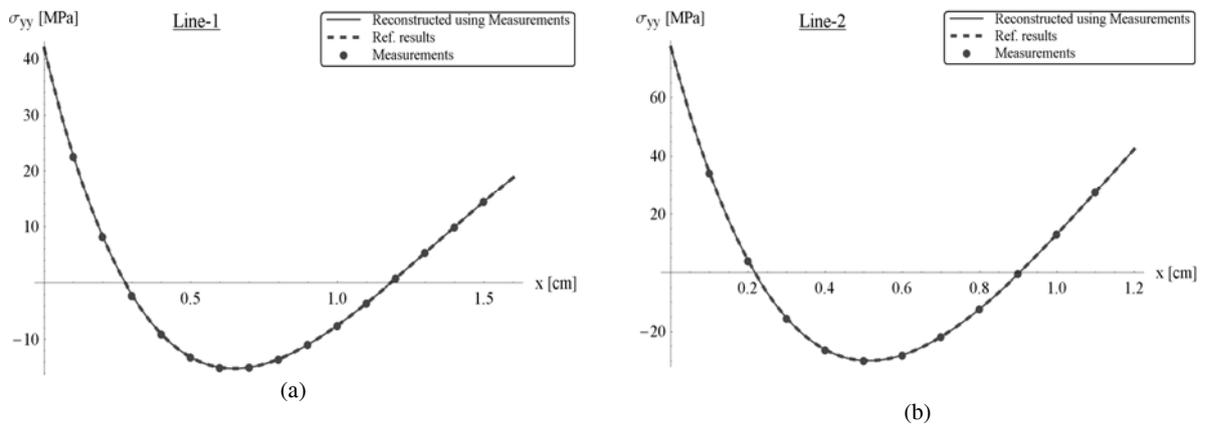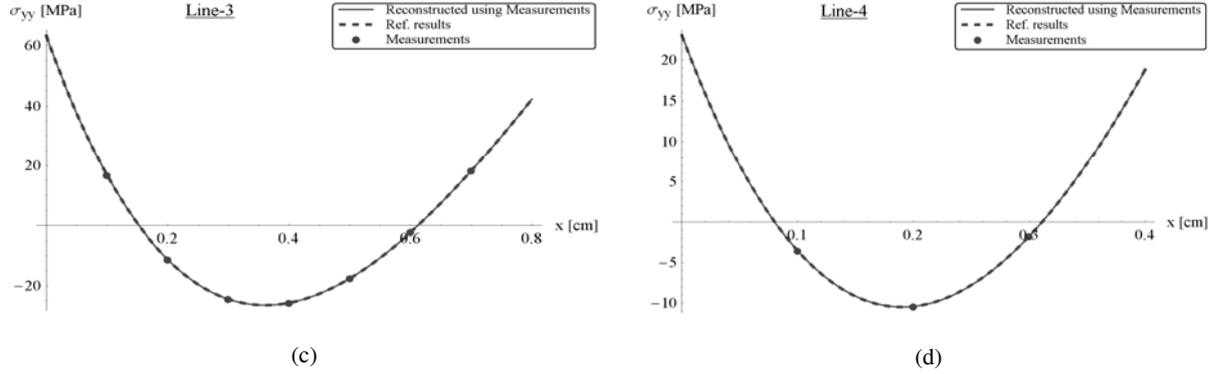
Fig. 5
"Measured" values and reference residual stress distribution compared to reconstructed longitudinal residual stress using "Measurements" along lines 1 through 4.

In reconstructing the residual stress field, the conditions of equilibrium equations, traction free boundary conditions and the constraint of a zero mean residual stress are satisfied. Furthermore , an optimal agreement between the measurements and model predictions was achieved in the least squares sense.

Figs. 7a-7b through Figs. 9a-9b compare two dimensional contour plots of the reference and reconstructed longitudinal residual stress, σ_{yy} , transversal residual stress, σ_{xx} , and shear residual stress, σ_{xy} , respectively, utilizing "Measured data". There is excellent agreement between the reconstructed and the reference residual stress field for the entire domain. It is worth noting that, the major component of the reference residual stress is σ_{xx} , and even when measured data are the residual stresses, σ_{yy} , there remains very good agreement in the entire domain and for all components.

The average mean of the error in reconstruction of residual stress utilizing "Measured data" with respect to the reference residual stress is defined as $\frac{1}{A}\iint_A \left| \sigma_{Rec}(x,y) - \sigma_{REF}(x,y) \right| dxdy$ where A is the area of the domain and $\sigma_{Rec}, \sigma_{REF}$ are the reconstructed and reference component of residual stress, respectively. The average value of the error in reconstruction of residual stresses using "Measured data" is found to be 5.99032 (MPa) for σ_{xx} and 0.25407 (MPa) for σ_{yy} and 0.86307 (MPa) for σ_{xy} , respectively.

Even utilizing the ideal "measured" residual stress results in an excellent agreement between the reconstructed and reference residual stress field but it is worth to study the sensitivity of the reconstructed solution to the data errors which is of the close interest of utilizing the present method in practice.

To this end, an acceptable practical absolute error, less than ±10% of the measurements [22], is randomly added to the "measured" data to make them more realistic. It should be noted that, by randomly it means that some "measured" data has positive and some other has negative absolute error. These "realistic measured" data are shown together with the "measured" values of the residual stress, σ_{yy} , and the reference residual stress distribution along lines 1 through 4 in Fig. 4.

The residual stress field is reconstructed again utilizing the "Realistic data" by the present method. When dealing with "Realistic data" that contain measurement error, it should be noted that; inverse problems are often ill-posed problems since the solutions need not depend continuously on "Realistic data" $T_k^{Real} = T_k \pm 0.1 \max\{T_k\}$. Similar to earlier work, [17] a Tikhonov-Morozov regularization method is introduced to reduce the measurement noise and smooth the stress solution. The regularization takes the output from the least squares formulation of the inverse problem and adds a stabilizing term to the least squares functional J, so that a solution $\{c(\alpha)\}$ is prescribed, where

$$J = \sum_{k=1}^{N} w_k \left(\sum_{i=1}^{P} \sum_{j=1}^{Q} c_{ij} \Upsilon_{ijk} - T_k^{Real} \right)^2 + \alpha \left(\sum_{i=1}^{P} \sum_{j=1}^{Q} c_{ij} \right)^2 \qquad (25)$$
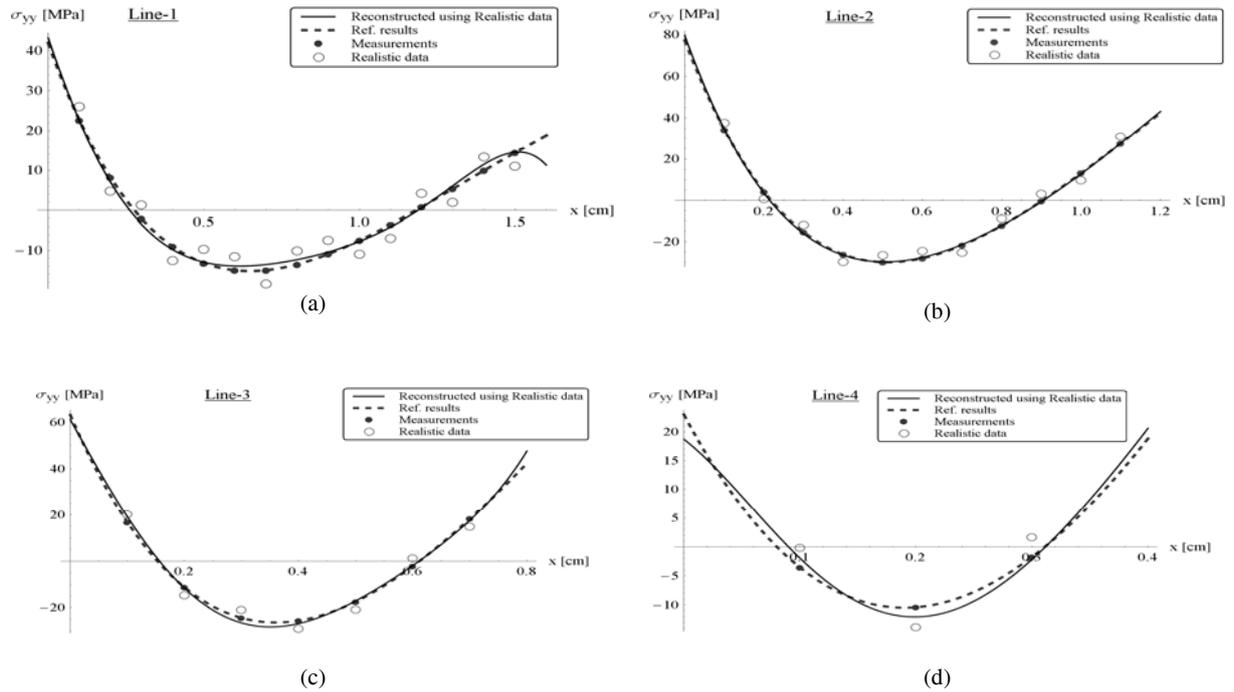
Fig. 6
"Realistic data" and reference residual stress distribution compared to reconstructed longitudinal residual stress using "Realistic data" along lines 1 through 4.

The parameter $\alpha > 0$, is known as the Tikhonov regularization parameter. To find the parameter, α, it is sufficient to utilize and solve the posteriori parameter choice strategy known as the discrepancy principle proposed by Morozov [21]. In the reconstructed results, utilizing "Realistic data" regularization method is used and also it is assumed that the noise level has the order of the maximum absolute errors in "Realistic data".

The reconstructed residual stresses utilizing "Realistic data" are shown in Fig. 6 and they are in a good agreement with the reference stress profile. The maximum error between the reconstructed residual stress using "Realistic data", σ_{yy}, and the reference profile is about 21.77% that occurs along line-4 and at the outer edge of the domain. However, it worth to note that, far from the edges of the domain, the regularized reconstructed stress field utilizing "Realistic data" has less error rather than the artificially introduced error, i.e. in interiors of domain the error is less than 10%.

Figs. 7c through Fig. 9c exhibit two dimensional contour plots of the reconstructed longitudinal residual stress, σ_{yy}, transversal residual stress, σ_{xx}, and shear residual stress, σ_{xy}, respectively, utilizing "Realistic data". There is good agreement between the reconstructed and the reference residual stress field for the entire domain.

The average mean of the error in reconstruction of residual stress utilizing "Realistic data" with respect to the reference residual stress is defined as $\frac{1}{A}\iint_A \left| \sigma_{Rec}^{Real}(x,y) - \sigma_{REF}(x,y) \right| dxdy$ where A is the area of the domain and σ_{Rec}^{Real}, σ_{REF} are the reconstructed using "Realistic data" and reference component of residual stress, respectively. The average value of the error in reconstruction of residual stresses using "Realistic data" is found to be 9.73323 (MPa) for σ_{xx} and 0.95349 (MPa) for σ_{yy} and 1.87513 (MPa) for σ_{xy}, respectively.
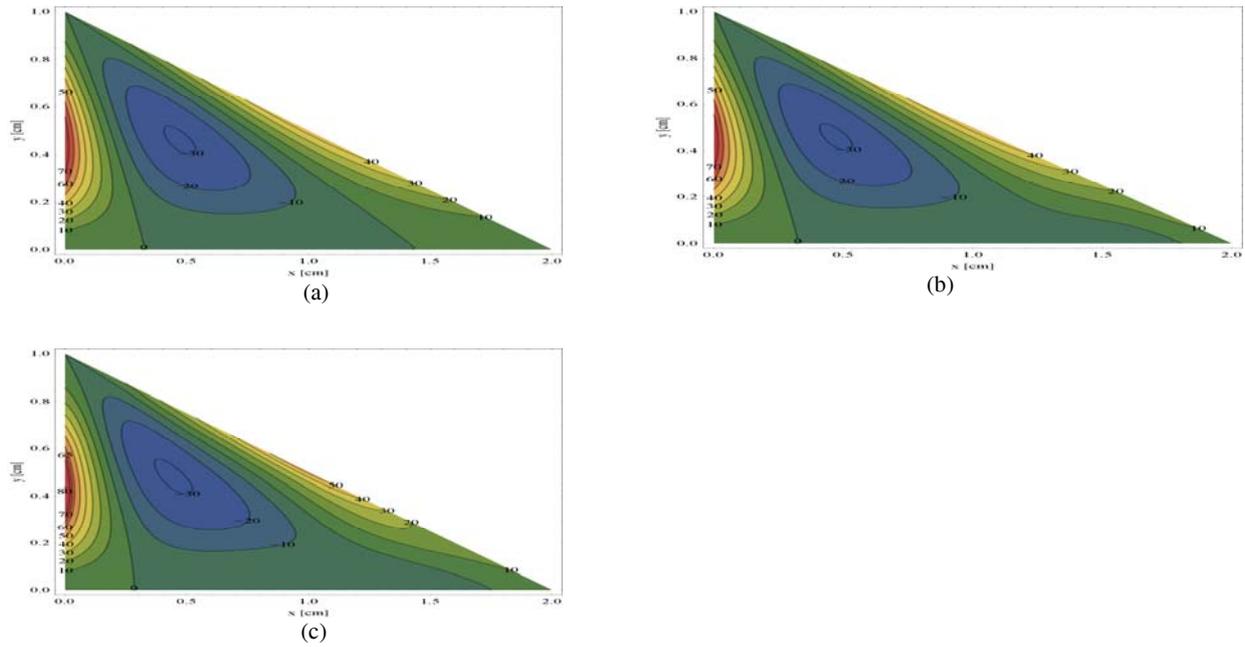
Fig. 7
Contour plot of the longitudinal residual stress component σ_{yy} a) reference solution b) reconstructed stress using "Measurements" c) reconstructed stress using "Realistic data".
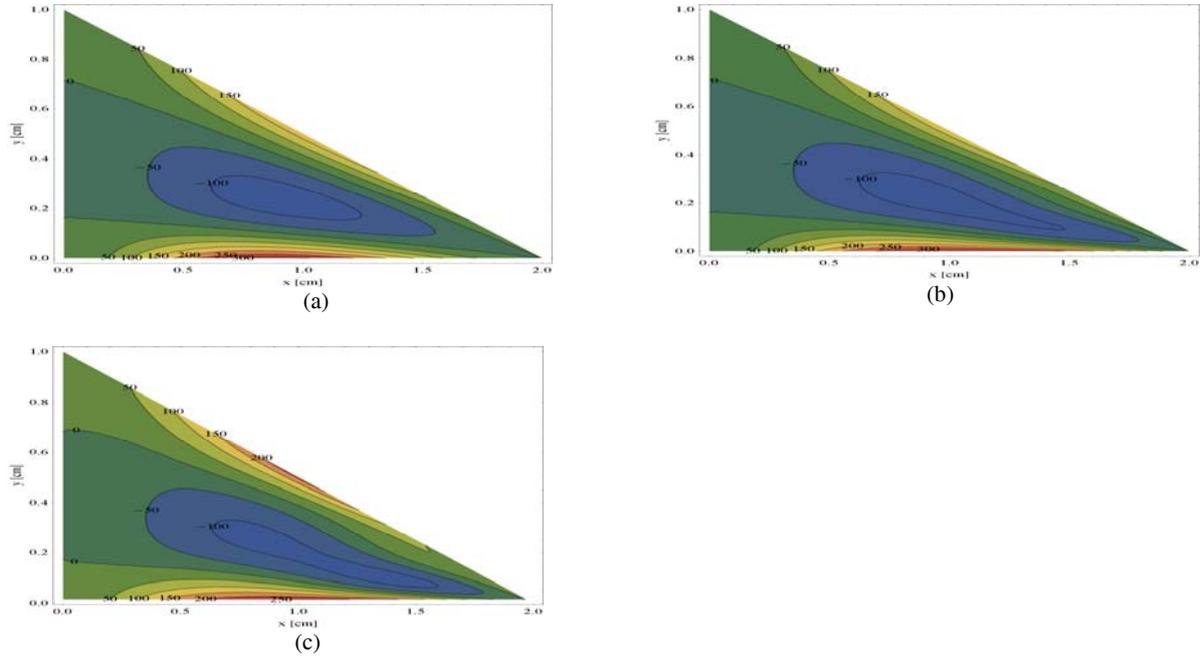
Fig. 8
Contour plot of the transversal residual stress component σ_{xx} a) reference solution b) reconstructed stress using "Measurements" c) reconstructed stress using "Realistic data".

(a)

(b)

(c)
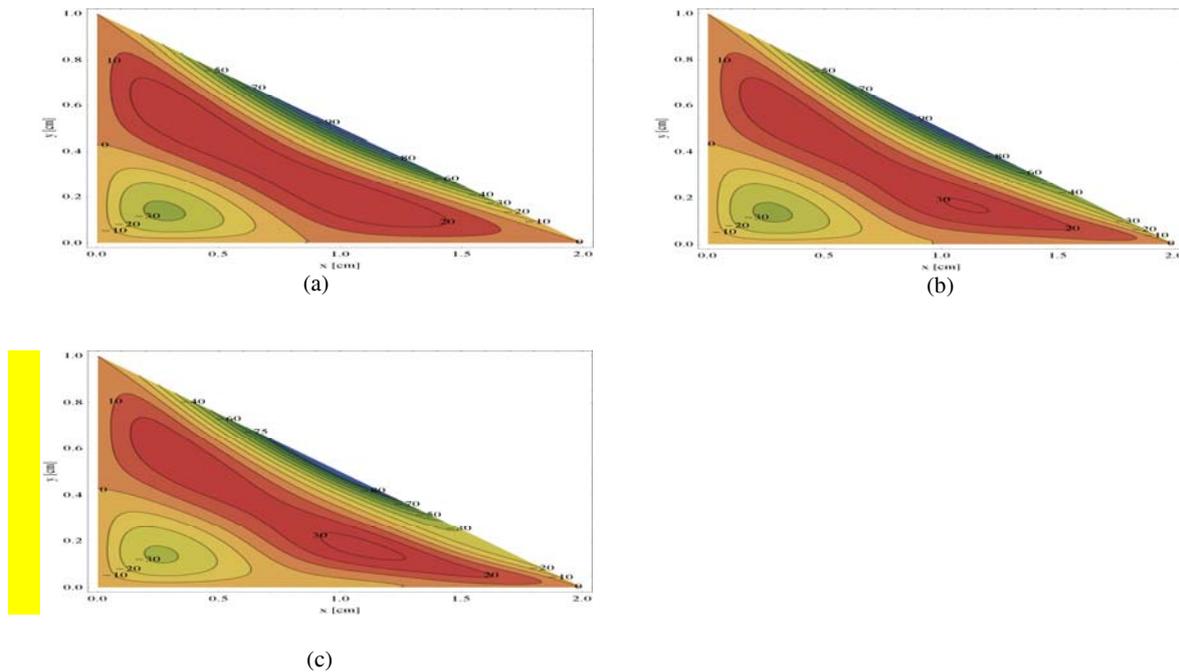
Fig. 9
Contour plot of the shear residual stress component σ_{xy} a) reference solution b) reconstructed stress using "Measurements" c) reconstructed stress using "Realistic data".

For each continuous function there is a corresponding formal expansion, i.e. Eq. (22), which has the property that partial sums are the best approximations to the function in the least squares sense. It can be shown mathematically that this partial sum in the least squares sense will always converge to the function under the conditions of linear independency of the shape functions. More mathematical details and discussion on approximation theory and regularization methods are given by Cheney [20] and Groetsch [21], respectively.

It is important to check that the shape functions $f_i(x)$ and $g_j(y)$ are linearly independent. To do this, the Wronskian determinant of each set of shape functions $f_i(x)$ and $g_j(y)$ is tested on the interval [0,a] and [0,b], respectively. For each set, it can be found at least one point where the Wronskian is not equal to zero; hence the set of shape functions must be linearly independent.

Also note that modified Chebyshev polynomials used as shape functions must be carefully considered. For example, the maximum order of these polynomials should not exceed the number of measurements, and then the shape functions according to Wronskian determinant will always be linear independent [23].

Thus far, it is shown that $f_i(x)$ and $g_j(y)$ are base functions in intervals [0,a] and [0,b], respectively; therefore the two dimensional shape functions $f_i(x)g_j(y)$ are also linear independent and act as the two dimensional base functions for the domain of $[0,a]\times[0,b]$ [24].

It is also important to study the rate and domain of convergence for the asymptotic solution. It is shown through Figs. 7-9 that utilizing the present analytical method, with truncated series with 10 terms in the *x*-direction and 7 terms in the *y*-direction, for both cases of reconstruction using either "Measured" values or "Realistic data", the solution has a fast convergence and has excellent agreement with the reference solution almost everywhere in the domain.

Also to check the accuracy of the numerical computations, a practical footnote for numerical computations is addressed here. The well-posedness of the reconstructed solution utilizing the present method is related to the condition number of the tensor Ψ_{ijmn} appearing in Eq. (19) and Eq. (20). If the condition number is small, where "small" means roughly the condition number to have the less order of the of tensor entries, then the numerical system is well-posed and has a well numerical behavior [25].

A key feature in this analytical reconstruction method of the residual stress throughout the domain is that it not only interpolates between measured data but also provides additional information. Furthermore, the possible stress fields included in the analysis are only those that satisfy all of the requirements for continuum mechanics. This results in significant additional constraints being placed on data interpretation. Provided the analysis of the measured data is performed using the proposed analytical procedure, all of the predicted residual stress fields necessarily conform to these constraints, furnishing additional insight into the residual stresses being studied. A further significant feature of the present study is that it not only enables us to minimize the error on one component and determine an expansion for that component, the analytical method also provides expansions for the other components of the residual stress field successfully.

4 CONCLUSIONS

An analytical solution is developed to reconstruct the residual stress field in an arbitrary convex polygon. The results and analysis provided in the present research exhibit that limited measurement data together with an appropriate airy stress function successfully provides a method of determining a complete residual stress field. Also the analysis of the sensitivity of the reconstructed solution to the data errors, which is of the close interest of experimental studies, is performed. It has been shown that utilizing the present method together with Tikhonov-Morozov regularization technique will results in stable reconstructed residual stress field. The approach thus provides a useful method for experimental residual stress analysis in complex domain, where typically the complete determination of the stress state at every point is often more difficult rather than the measurement of only one component of stress. This new analytical approach for determination of the residual stresses has the potential to provide significant improvement in the quality of data interpretation of the residual stress measurements.

REFERENCES

[1]   Smith D.J., Farrahi G.H., Zhu W X., McMahon C.A., 2001, Obtaining multiaxial residual stress distributions from limited measurements, *Materials Science and Engineering A* **303**: 281–291.

[2]   Hill M.R., 1996, *Determination of residual stress based on the estimation of eigenstrain*, Ph.D. Thesis. Stanford University.

[3]   Cao Y.P., Hu N., Lu J., Yao Z.H., 2002, An inverse approach for constructing residual stress field induced by welding, *Journal of Strain Analysis for Engineering Design* **37**: 345–359.

[4]   Qian X., Yao Z., Cao Y., Lu J., 2005, An inverse approach to construct residual stresses existing in axisymmetric structures using BEM, *Journal of Engineering Analysis with Boundary Elements* **29**: 986–99.

[5]   Korsunsky A.M., Regino G.M., Nowell D., 2007, Variational eigenstrain analysis of residual stresses in a welded plate, *International Journal of Solids and Structures* **44(13)**: 4574–4591.

[6]   Jun T.S., Korsunsky A.M., 2010, Evaluation of residual stresses and strains using the eigenstrain reconstruction method, *International Journal of Solids and Structures* **47**:1678–1686.

[7]   Ballard P., Constantinescu A., 1994, On the inversion of subsurface residual stresses from surface stress measurements, *Journal of the Mechanics and Physics of Solids* **42(11)**: 1767-1787.

[8]   Schajer G.S., Prime M.B., 2006, Use of inverse solutions for residual stress measurements, *Journal of Engineering Materials and Technology* **128**: 375-382.

[9]   Hoger A., 1986, On the determination of residual stress in an elastic body, *Journal of Elasticity* **16**: 303-324.

[10]   Mura T., Gao Z., 1991, Inverse method in micromechanics of defects in solids, *Proceedings of the 3rd International Conference on Residual Stress* 1157-1167.

[11]   Robertson R.L., 1998, Determining residual stress from boundary measurements: a linearized approach, *Journal of Elasticity* **52**: 63–73.

[12]   Moore M.G., Evans W.P., 1958, Mathematical correction for stress in removed layers in X-ray diffraction residual stress analysis, *S A E Transactions* **66**: 340-345.

[13]   Faghidian S.A., 2010, *Estimation of Residual Stress Field Using Limited Measurements*, Ph.D. Thesis. Sharif University of Technology, Tehran, Iran.

[14]   Farrahi G.H., Faghidian S.A., Smith D.J., 2009, An inverse approach to determination of residual stresses induced by shot peening, *International Journal of Mechanical Science* **51**: 726–731.

[15]   Farrahi G.H., Faghidian S.A., Smith D.J., 2009, Reconstruction of residual stresses in autofrettaged thick-walled tubes from limited measurements, *International Journal of Pressure Vessel and Piping* **86**: 777-784.

[16]   Farrahi G.H., Faghidian S.A., Smith D.J., 2009, A new analytical approach to reconstruct residual atresses due to turning Process, *Proceeding of World Academy of Science Engineering and Technology* **55**: 453-457.

[17]   Farrahi G.H., Faghidian S.A., Smith D.J., 2010, An inverse method for reconstruction of the residual stress field in welded plates, *Journal of Pressure Vessel Technology - Transactions of the ASME* **132**: 061205-1:9.

[18]   Faghidian S.A., Goudar D., Farrahi G.H., Smith D.J., 2011, Measurement analysis and reconstruction of residual stresses, *Journal of Strain Analysis for Engineering Design* **47(4)**: 254-264.

[19]   Gurtin M.E., 1972, *The Linear Theory of Elasticity*, Handbuch der Physik, Vol. VIa/2. Springer-Verlag, Berlin.

[20]   Cheney E.W., 1982, *Introduction to Approximation Theory*,American Mathematical Society, Chelsea Publishing, New York.

[21]   Groetsch C.W., 2007, *Stable Approximate Evaluation of Unbounded Operators*, Springer, Berlin.

[22]   Kandil F.A., Lord J.D., Fry A.T., Grant P.V., 2001, *A Review of Residual Stress Measurement Methods a Guide to Technique Selection,* MATC (A) 04, UK National Physical Laboratory (NPL) Materials Centre report .

[23]   King A.C., Billingham J., Otto S.R., 2003, *Differential Equations: Linear, Nonlinear, Ordinary, Partial*. Cambridge University Press, Cambridge.

[24]   Hirota R.Y., 2004,*The Direct Method in Soliton Theory*, Cambridge University Press, Cambridge.

[25]   Demmel J.W., 1997, *Applied Numerical Linear Algebra*, SIAM (Society for Industrial and Applied Mathematics), Philadelphia.